Electronic Supplementary Material (ESI) for Energy & Environmental Science.

Supplementary Information for

Solution-Processed, Mercaptoacetic Acid-Engineered CdSe Quantum Dots Photocathode for Efficient Hydrogen Production under Visible Light Irradiation

Bin Liu†, Xu-Bing Li†, Yu-Ji Gao, Zhi-Jun Li, Qing-Yuan Meng, Chen-Ho Tung, and Li-Zhu Wu*

Key Laboratory of Photochemical Conversion and Optoelectronic Materials, Technical Institute of Physics and Chemistry & University of Chinese Academy of Sciences, the Chinese Academy of Sciences, Beijing 100190, P. R. China

†The two authors contributed equally to this work.

*To whom correspondence should be addressed. *E-mail:* lzwu@mail.ipc.ac.cn,

Telephone: (+86) 10-8254-3580*, Fax:* (+86) 10-8254-3580

A Table of Contents

Supplementary Fig. 1

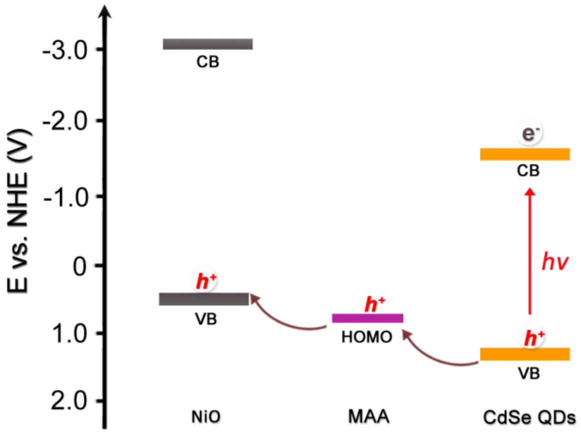

Figure S1. The Energy diagram of NiO, CdSe QDs and the linker of MAA is demonstrated to illustrate the feasibility of charge transfer at the interface of CdSe/NiO photocathode.

Supplementary Fig. 2

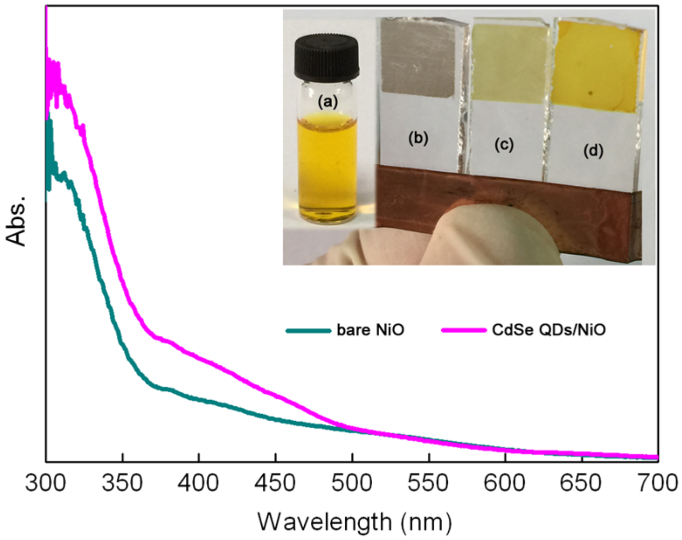

Figure S2. UV-Vis absorption spectra of bare NiO mesoporous film electrode (dark cyan line) and the assembled CdSe QDs/NiO electrode (pink line). According to the UV-Vis diffuse reflectance spectra of bare NiO, the band gap of NiO is estimated to be ~3.5 eV, which is highly consistent with the literature reported value.[1, 2] Insert: photographs of CdSe QDs colloidal solution (a), NiO electrode (b), CdSe QDs/NiO electrode (c) and CdSe QDs/TiO_2 electrode (d).

Supplementary Fig. 3

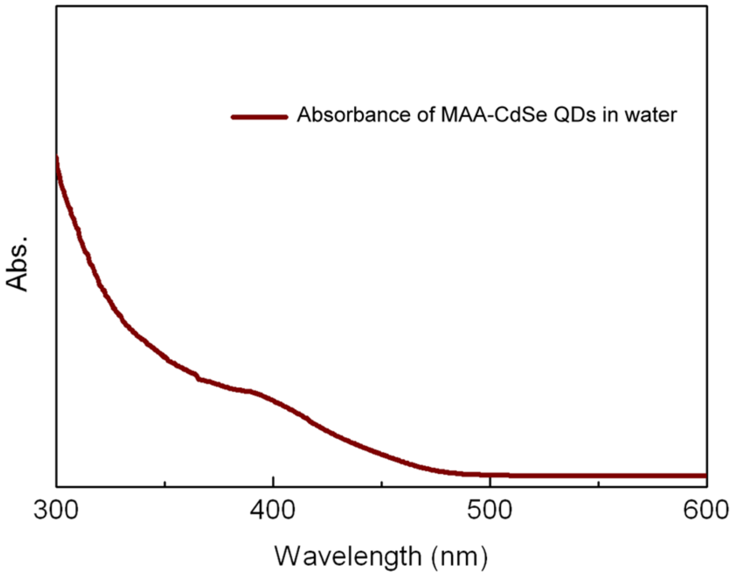

Figure S3. UV-Vis absorption spectrum of MAA-CdSe QDs is obtained in aqueous solution at low concentration. According to the UV-Vis spectrum of free CdSe QDs in aqueous solution, the band gap of CdSe QDs (2.0 nm in diameter) is determined to be ~2.65 eV.

Supplementary Fig. 4

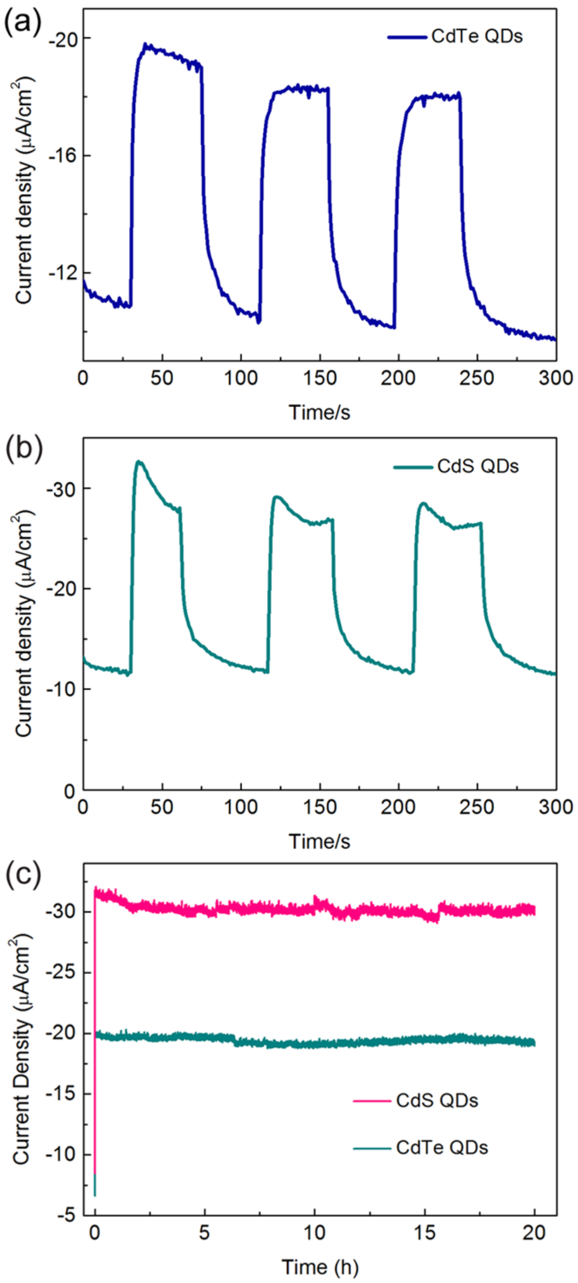

Figure S4. The transient photocurrent responses to on-off illumination of the linker-engineered (a) CdTe QDs/NiO electrode and (b) CdS QDs/NiO electrode in 0.1 M Na_2SO_4 solution (pH 6.8) at -0.1 V *vs.* NHE**.** And (c) J-t curves of the assembled CdS QDs/NiO electrode and CdTe QDs/NiO electrode in a 20-h test by taking the sample photoelectrode (0.64 cm^2) as working electrode, Ag/AgCl (3.0 M KCl) as reference electrode, platinum sheet as counter electrode (5 mm × 20 mm), and 0.1 M Na_2SO_4 as electrolyte at pH 6.8.

Supplementary Fig. 5

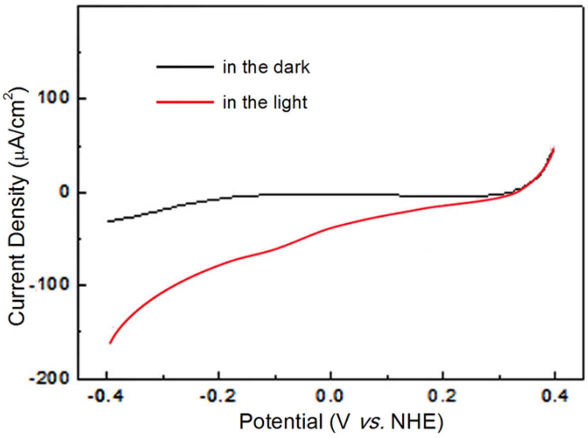

Figure 5. Current-potential curves of the CdSe QDs/NiO photocathode obtained in the dark and under visible light irradiation (100 mW/cm^2) by taking the sample photoelectrode (0.64 cm^2) as working electrode, Ag/AgCl (3.0 M KCl) as reference electrode, platinum sheet as counter electrode (5 mm × 20 mm), and 0.1 M Na_2SO_4 as electrolyte under 300 W Xe lamp illumination (~100 mW cm^{-2}) with a UV filter.

Supplementary Fig. 6

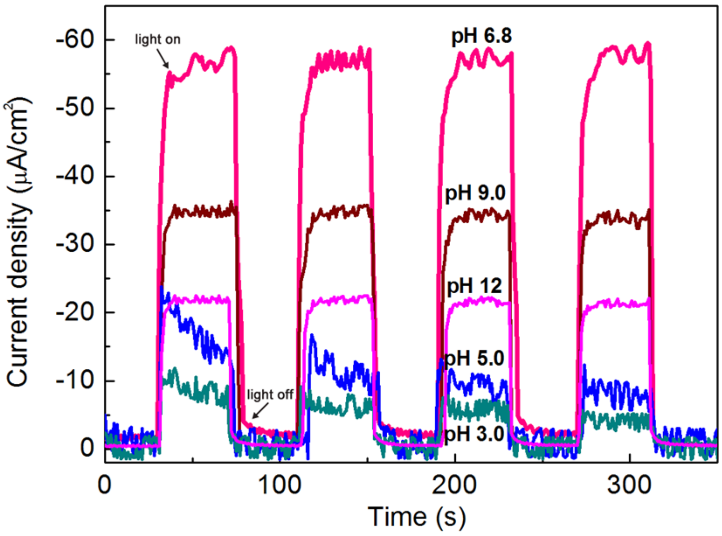

Figure S6. The PEC measurements were carried out in a water splitting setup, consisting of the sample photoelectrode (0.64 cm^2) as working electrode, Ag/AgCl (3.0 M KCl) as reference electrode, platinum sheet as counter electrode (5 mm × 20 mm), and 0.1 M Na_2SO_4 as electrolyte at different pH values (adjusted by H_2SO_4 or NaOH solution). Light irradiation: 300 W Xe-lamp illumination (~100 mW cm^{-2}) with a UV filter; applied bias of -0.1 V *vs.* NHE.

Supplementary Fig. 7

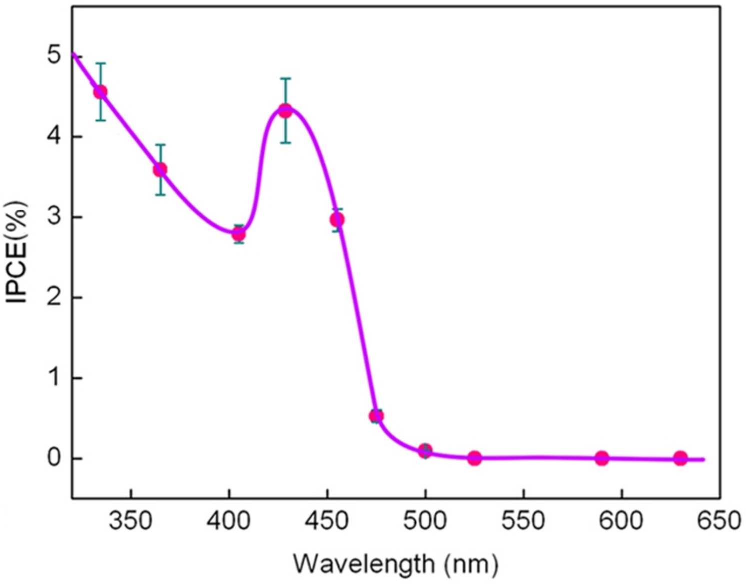

Figure S7. IPCE spectrum of the assembled CdSe QDs/NiO photocathode was obtained in 0.1 M Na_2SO_4 aqueous solution at pH 6.8 with an applied bias of -0.1 V *vs.* NHE**.** Error bars represent mean ±s.d. of three independent experiments.

Supplementary Fig. 8

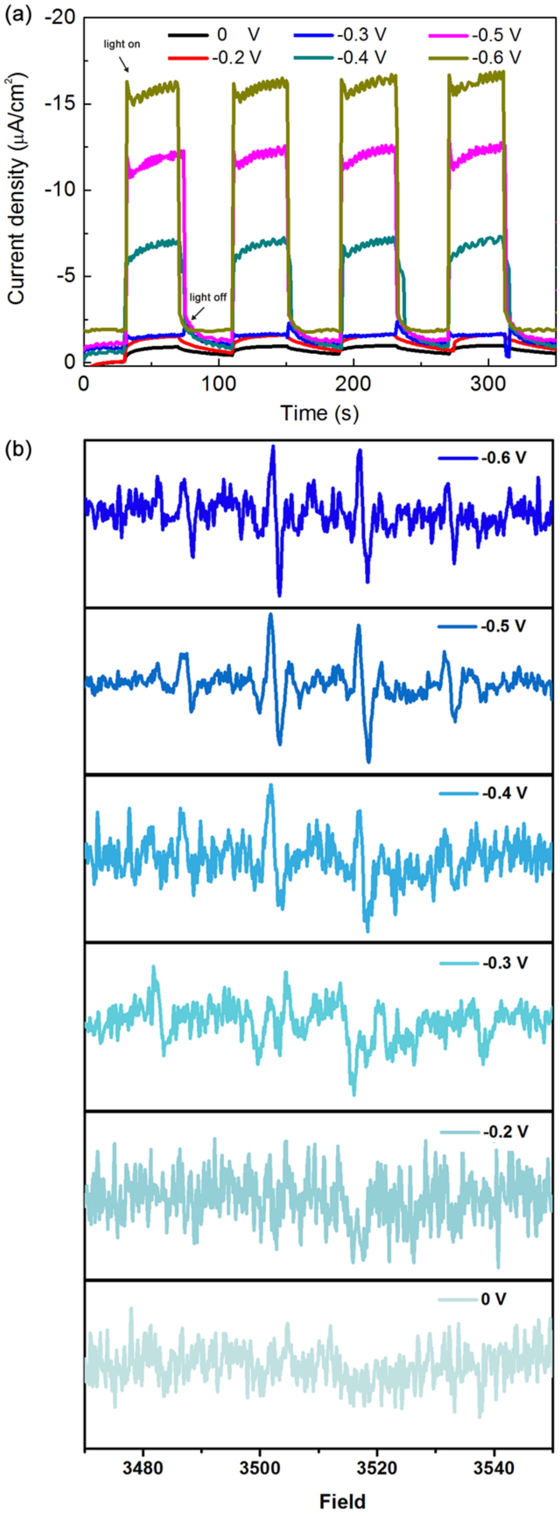

Figure S8. (a) The transient photocurrent responses to on-off illumination at different applied bias of a two-electrode PEC system and (b) the corresponding EPR spectra of trapped ·OH radicals after 2.5 h test by using DMPO (0.02 M) as a trapping reagent.

Supplementary Fig. 9

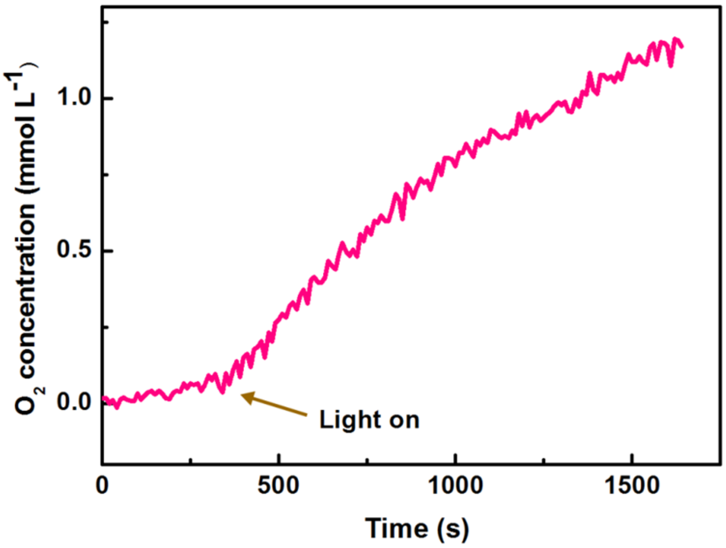

Figure S9. O_2 evolution was directly observed by using an Ocean Optics fluorescence-based oxygen sensor. The oxygen evolution was carried out in a sealed water splitting setup under inert atmosphere (Argon), consisting of the sample photoelectrode as working electrode, Ag/AgCl (3.0 M KCl) reference electrode, and platinum sheet counter electrode in 20 mL 0.1 M Na_2SO_4 as electrolyte at pH 6.8. The needle probe was inserted through a rubber septum and continuously monitored O_2 evolution throughout the PEC operation. The experiment began with 3.0 h of baseline before O_2 measurement followed by illumination using 410 nm LEDs (100 mW cm^{-2}) and -0.1 V (*vs.* NHE) applied bias.

Supplementary Fig. 10

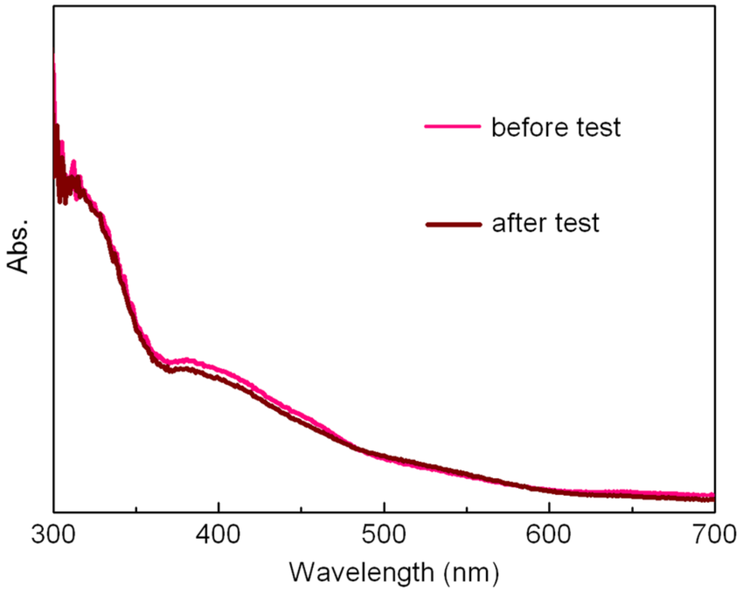

Figure S10. DRS spectra of the assembled CdSe QDs/NiO photocathode obtained before (pink line) and after (wine line) 45-h test under the three-electrode PEC condition.

Supplementary Fig. 11

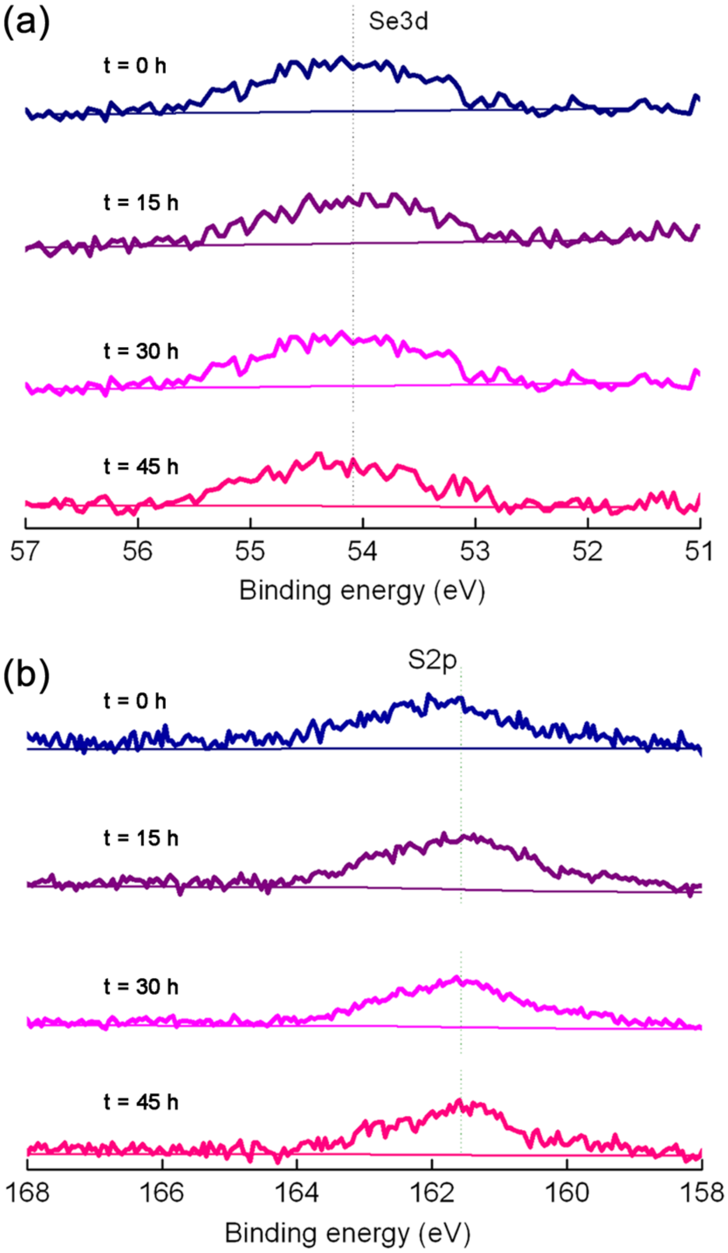

Figure S11. Se3d (a) and S2p (b) XPS spectra of the assembled CdSe QDs/NiO electrode at the different PEC operation times of 0 h, 15 h, 30 h, 45 h, respectively, from top to bottom.

Supplementary Fig. 12

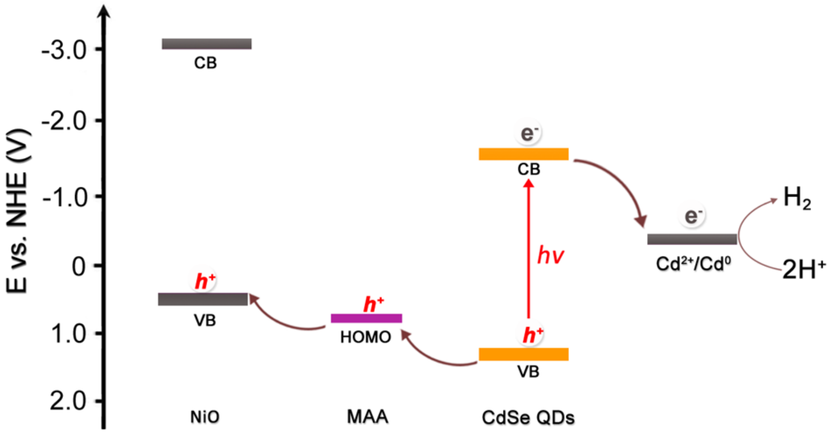

Figure S12. The Energy diagram of NiO, CdSe QDs, surface cadmium and the linker of MAA at the interface of CdSe/NiO photocathode and the corresponding mechanism for PEC H_2 evolution are provided.

Supplementary Fig. 13

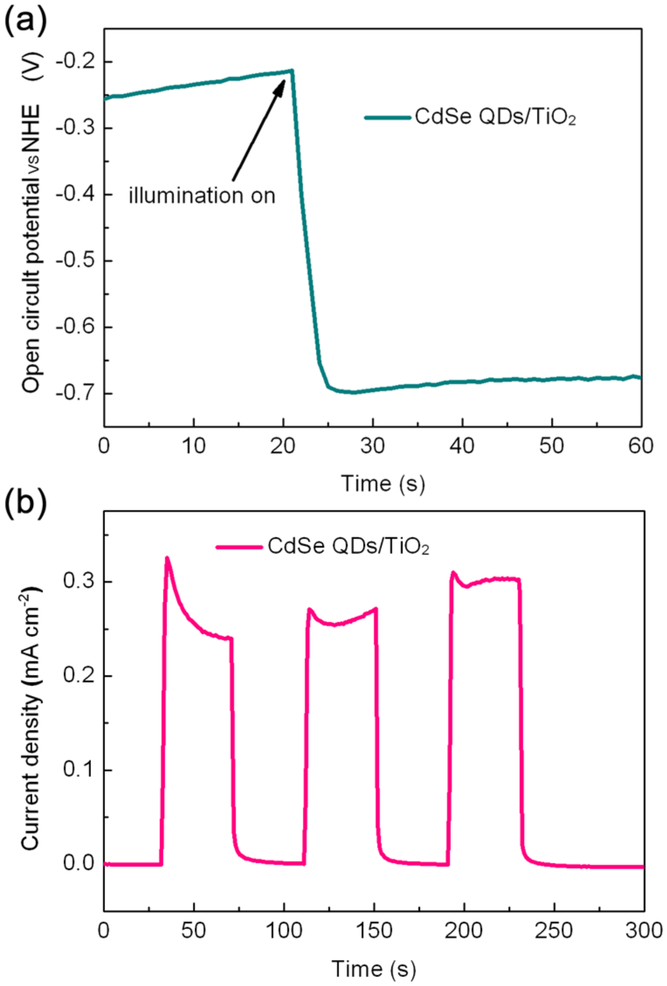

Figure S13. (a) The open circuit potential (OCP) response under visible light irradiation for CdSe QDs sensitized TiO_2 film electrode; (b) the transient photocurrent responses to on-off illumination of CdSe QDs sensitized TiO_2 film electrode.

Supplementary Fig. 14

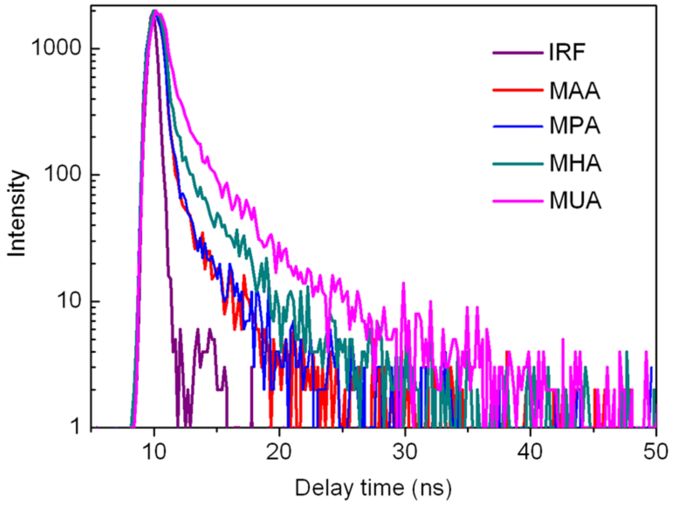

Figure S14. Photoluminescence decays of CdSe QDs/NiO electrodes assembled by MAAs with different alkyl chain length.

Supplementary Fig. 15

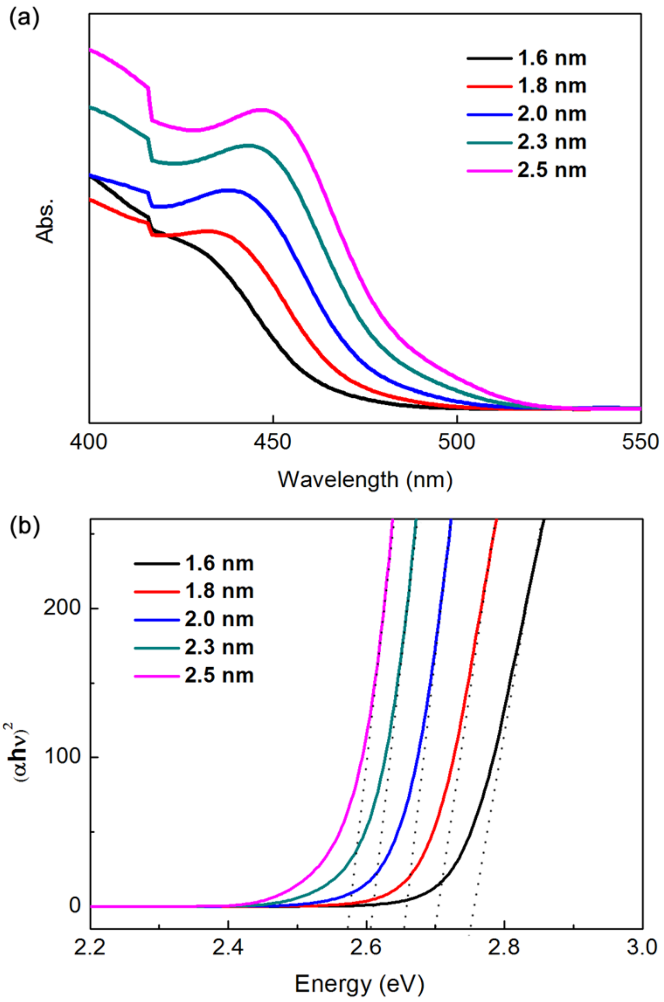

Figure S15. (a) The UV-Vis absorption spectra and (b) corresponding Tauc plots of MAA-CdSe QDs obtained at different reaction times, indicating an increase of band gap (~2.58 eV to 2.75 eV) and average size from 1.6 nm to 2.5 nm calculated bv using Peng's method. The Tauc plots are obtained according to the equ $(\alpha h\nu)^2 = C_1(h\nu - E_g)$

Where *α* is the linear absorption coefficient of the material, *hv* is the photon energy and C_1 is a proportionality constant.

Supplementary 16

Table S1 Monitoring the pH variation during a long term PEC measurement:

Time/h	0	12	24	40
pH	6.80	6.79	6.82	6.90

Note: the PEC measurements were carried out in a water splitting setup, consisting of the sample photoelectrode (0.64 cm^2) as working electrode, Ag/AgCl (3.0 M KCl) as reference electrode, and platinum sheet as counter electrode (5 mm × 20 mm) and 0.1 M Na_2SO_4 as electrolyte at pH 6.8. Light irradiation: 300 W Xe lamp illumination (~100 mW cm^{-2}) with a UV filter; applied bias: -0.1 V *vs.* NHE.

17. Chemicals

NiO powder (< 50 nm), Mercaptoacetic acid (MAA, 99%), 3-Mercaptopropionic acid (MPA, 99%), 6-Mercaptohexanoic acid (MHA, 99%), 11-Mercaptoundecanoic acid (MUA, 99%), selenium powder (about 200 mesh), $CdCl_2 \cdot 5/2H_2O$ (99%) and ethanolic ethylcellulose were purchased from Sigma-Aldrich. Terpineol was purchased from TCI. Other chemicals are of analytical grade without further purification unless otherwise noted. The ultrapure water with 18.2 MΩ cm (Mettler Toledo, FE20, China) was used thorough the experiment.

18. Synthesis of MAA-CdSe QDs and fabrication of photocathode

Synthesis of MAA-CdSe QDs: an aqueous solution of colloidal MAA-CdSe QDs was synthesized by the reaction between Cd^{2+} and Na_2SeSO_3 according to the method described in our previous work.[4] In detail, Cd^{2+} precursor was prepared by mixing a solution of $CdCl_2 \cdot 5/2H_2O$ (46.0 mg, 0.20 mM) and MAA (26 μL, 0.30 mM) in 190 mL ultrapure water. The pH value was then adjusted to 11.0 by 1.0 M NaOH. Deaerated with N_2 bubbling for 30 min, 10.0 mL freshly prepared Na_2SeSO_3 solution (5.0 mM) was added into the above solution. Aliquots of the reaction solution were taken out at regular intervals for characterization by UV-Vis absorption and emission. The diameter of the obtained MAA-CdSe QDs was calculated by Peng's method[5] and verified by high resolution TEM characterization. A range of 1.6 to 2.5 nm in diameter of MAA-CdSe QDs has been obtained by refluxing for different time 0-12 h.

Preparation of NiO mesoporous film electrode: NiO mesoporous film electrode was fabricated following the reported method.[6] In brief, an aqueous suspension of commercially available NiO nanoparticles (mean size below 50 nm) was printed on FTO substrate using a semiautomatic screen printer. FTO substrate with aqueous suspension film of NiO was then sintered at 450 °C for 2.0 hour under air atmosphere, and then the NiO mesoporous film electrode was obtained after being cooled to room temperature.

Fabrication of MAA-engineered CdSe QDs/NiO electrode: A concentrated solution of 5.0 mL as-prepared MAA-CdSe QDs (2.0×10^{-4} M) was precipitated by adding 0.1 M hydrochloric acid until QDs aggregated and then the precipitate was separated by centrifugation (7000 rpm, 6 min) to remove the residual ligands in solution and surface bonded stabilizers. The obtained precipitate was then redispersed in 5.0 mL MAA solution (0.23 mmol) at pH 11.0 to form a transparent bright-yellow stock solution (2.0×10^{-4} M). Subsequently, a NiO mesoporous film electrode prepared above was soaked in the stock solution for 4.0 hours. Then washed with ultrapure water for at least three times and dried under air, the colloidal CdSe QDs sensitized NiO mesoporous film electrode was obtained by using MAA as a linker. Similar procedures were applied for the preparation of other MAAs (just replacing MAA with same amount of MPA, MHA or MUA) molecules to fabricate the assembled CdSe QDs/NiO electrodes.

19. Characterization and measurement

The UV-Vis diffuse reflectance spectra (UV-Vis DRS) were recorded by Cary 5000 UV-visible-NIR spectrophotometer employing a lab-sphere diffuse reflectance accessory in the range of 200-2000 nm. The UV-Vis spectra of the colloid CdSe QDs were measured in quartz cuvettes (optical path = 1 cm) with a Shimadzu UV-1601PC spectrophotometer. High-resolution transmission electron microscopy (HRTEM) was performed by JEM 2100F (operated at an accelerating voltage of 200 kV). The morphologies and energy dispersive X-ray (EDX) mapping of the electrodes were examined by a HITACHI S-4800 scanning electron microscope (SEM) equipped with an energy dispersive spectrometer (accelerating voltage of 15 kV). Element content was determined by an inductively coupled plasma mass spectroscopy (ICP, Varian 710-ES). The chemistry state of elements was evaluated by X-Ray photoelectron spectroscopy instrument (XPS, ESCALAB 250 spectrophotometer with Al-Kα radiation) and all the binding energies are calibrated with C $sp^2 1s$ at 284.6 eV. Time-resolved emission decay was measured by time-correlated single photon counting (Edinburgh Instruments, FLS-920) with laser (405 nm) as the excitation light source. Photoelectrochemistry measurement was carried out in a three-electrode setup with the working electrode of the sample film electrode, counter electrode of platinum disk, and reference electrode of Ag/AgCl (3.0 M KCl). An aqueous solution of $Na_4[Fe(CN)_6]$ (1.0 mM) was used to determine the potential of the reference electrode ($E_{Ag/AgCl}$ = +0.194 V *vs.* NHE). The electrolyte (0.1 M Na_2SO_4, pH = 6.8) was degassed for 120 minutes by flushing high purity argon prior to and during each measurement. For photocurrent measurement, the light source was a 300 W Xe-lamp with a UV cut-off filter unless otherwise stated; the light intensity at the surface of the electrode is 100 mW cm^{-2}. Prior to measurement, the area of the electrode was fixed by insulating cement and the exposed area was 0.64 cm^2. A

Zennium electrochemical workstation (Germany, Zahner Company) was used. The transient photocurrent response to on-off illumination was performed when the sample electrode was applied a constant potential (-0.1 V *vs.* NHE). Open circuit potential curve was recorded under on-off illumination. Stability test was performed by chronoamperometry. A constant potential (-0.1 V *vs.* NHE) was applied to the electrode for a period of 45 h while the current density was recorded. The produced hydrogen was measured using a gas chromatography with CH_4 as internal standard for quantitative analysis, and the evolved oxygen was measured with an Ocean Optics fluorescence-based oxygen sensor. IPCE was measured under monochromatic light irradiation provided by the xenon lamp equipped with band pass filters. The light intensity was tested with a Newport photometer.

20. The size and extinction coefficient (ε) of CdSe QDs

The size (*D*) and extinction coefficient (ε) of the CdSe QDs can be determined according to following equations (S1-S3),

$$A = \varepsilon CL \tag{S1}$$

$$\begin{aligned} D = {} & (1.6122\times10^{-9})\lambda^4 - (2.6575\times10^{-6})\lambda^3 \\ & + (1.6242\times10^{-3})\lambda^2 - (0.4277)\lambda + (41.57) \end{aligned} \tag{S2}$$

$$\varepsilon = 5857(D)^{2.65} \tag{S3}$$

where, *A* is the absorbance at the first excitonic peak of CdSe QDs; *C* is the molar concentration (mol L^{-1}) of CdSe QDs; *L* is the path length (cm) of the radiation beam; *D* (nm) is the size of CdSe QDs; λ is the wavelength of the first absorption peak (from low energy) of CdSe QDs; ε is the extinction coefficient of CdSe QDs.

21. Analysis of the time-resolved PL decays of CdSe QDs

The excited CdSe deactivation was investigated by monitoring the photoluminescence decay as previously reported elsewhere.[7] Multi-exponential decay kinetics model can be used to fit the photoluminescence decay to determine the photoluminescence lifetimes for CdSe QDs. Then, the average lifetime of CdSe photoluminescence decay can be estimated according to the equation (S4),

$$\langle \tau \rangle = \frac{\sum_{i=1}^{n} \alpha_i \tau_i^2}{\sum_{i=1}^{n} \alpha_i \tau_i} \qquad \text{(S4)}$$

Where, α_i and τ_i items respectively represent the individual pre-exponential and the lifetime terms, $<\tau>$ represent the average lifetime.

22. Kinetic parameters of CdSe QDs photoluminescence decay analysis

Assuming that the observed decrease in lifetime is attributed to the hole transfer to NiO, we can estimate the hole-transfer rate constant by the equation (S5),

$$k_{et} = \frac{1}{\langle \tau_{CdSe-NiO} \rangle} - \frac{1}{\langle \tau_{CdSe-SiO_2} \rangle} \qquad \text{(S5)}$$

Where, $<\tau_{\text{CdSe-NiO}}>$ and $<\tau_{\text{CdSe-SiO}_2}>$ are the average lifetime of CdSe QDs measured on NiO and SiO_2, respectively. The kinetic parameters of the CdSe photoluminescence decay analysis are listed in the following table (S1).

Table S2. Kinetic parameters of CdSe QDs photoluminescence decay analysis.

	α_1	τ_1 /ns	α_2	τ_2 /ns	α_3	τ_3 /ns	$<\tau_a>$ /ns
CdSe on SiO_2	45.03	1.0	34.23	5.8	20.7	32	9.1
CdSe on NiO	84.67	1.8	15.33	4.9			2.3

23. IPCE measurement

IPCE measurement was carried out in a three-electrode setup with the working electrode of the sample film electrode, counter electrode of platinum disk, and reference electrode of Ag/AgCl (3.0 M KCl). IPCE was calculated according to equation (S6),[8]

$$\mathrm{IPCE}\left(\%\right)=\frac{1240J}{\lambda\times I}\times 100\% \qquad \text{(S6)}$$

Where, J represents the photocurrent density (mA cm^{-2}), λ is the wavelength of incident light (nm), and I is the intensity of the incident light (mW cm^{-2}).

24. Faradic efficiency

In a 12 h PEC measurement, 0.335 C charge carriers passed through the external circuit; simultaneously ~1.74 μmol of molecular H_2 was detected by gas chromatography. Herein, the Faradic efficiency was calculated according to the following equation (S7):

$$\eta = \frac{\text{amount of } H_2 \text{ (mol)}}{\text{amount of e/2 (mol)}} \times 100\% = 100\% \quad \text{(S7)}$$

25. Marcus-type expression for charge-transfer

The hole (or electron) charge-transfer rate can be determined according to the following equation (S8),[9]

$$k_{ET} = \left(\frac{\pi}{\lambda k_B T}\right)^{1/2} \frac{V^2}{\hbar} \exp\left(-\frac{\lambda}{4 k_B T}\right) \qquad \text{(S8)}$$

Where, T is the temperature, k_B the Boltzmann constant, $\hbar$ the Planck constant, λ the reorganization energy accompanying geometric relaxation associated with the charge transfer and V the effective electronic coupling matrix element between neighboring species, dictated largely by orbital overlap.

26. References

1. G. Boschloo and A. Hagfeldt, *J. Phys. Chem. B*, 2001, **105**, 3039-3044.
2. L. Tong, A. Iwase, A. Nattestad, U. Bach, M. Weidelener, G. Gotz, A. Mishra, P. Bauerle, R. Amal, G. G. Wallace and A. J. Mozer, *Energy Environ. Sci.*, 2012, **5**, 9472-9475.
3. A. Hagfeldt and M. Grätzel, *Chem. Rev.*, 1995, **95**, 49-68.
4. Z.-J. Li, J.-J. Wang, X.-B. Li, X.-B. Fan, Q.-Y. Meng, K. Feng, B. Chen, C.-H. Tung and L.-Z. Wu, *Adv. Mater.*, 2013, **25**, 6613-6618.
5. W. W. Yu, L. Qu, W. Guo and X. Peng, *Chem. Mater.*, 2003, **15**, 2854-2860.
6. A. Nattestad, A. J. Mozer, M. K. R. Fischer, Y. B. Cheng, A. Mishra, P. Bauerle and U. Bach, *Nat. Mater.*, 2010, **9**, 31-35.
7. A. Kongkanand, K. Tvrdy, K. Takechi, M. Kuno and P. V. Kamat, *J. Am. Chem. Soc.*, 2008, **130**, 4007-4015.
8. H. M. Chen, C. K. Chen, R.-S. Liu, L. Zhang, J. Zhang and D. P. Wilkinson, *Chem. Soc. Rev.*, 2012, **41**, 5654-5671.
9. G. R. Hutchison, M. A. Ratner and T. J. Marks, *J. Am. Chem. Soc.*, 2005, **127**, 16866-16881.